Int. J. Bio-Inorg. Hybr. Nanomater., 5(2): 105-113, Summer 2016

NH_3 sensors based on novel TiO_2/MoS_2 nanocomposites: Insights from density functional theory calculations

A. Abbasi [1,2,3]; J. Jahanbin Sardroodi [1,2,3]*

[1] Molecular Simulation Laboratories (MSL), Azarbaijan Shahid Madani University, Tabriz, Iran
[2] Computational Nanomaterials Research Group, Azarbaijan Shahid Madani University, Tabriz, Iran
[3] Department of Chemistry, Faculty of Basic Sciences, Azarbaijan Shahid Madani University, Tabriz, Iran

Received: 1 March 2016; Accepted: 4 May 2016

ABSTRACT: Density functional theory calculations were performed to investigate the interactions of NH_3 molecules with TiO_2/MoS_2 nanocomposites in order to completely exploit the adsorption properties of these nanocomposites. Given the need to further comprehend the behavior of the NH_3 molecules oriented between the TiO_2 nanoparticle and MoS_2 monolayer, we have geometrically optimized the complex systems consisting of the NH_3 molecule positioned at appropriate sites between the nanoparticle and MoS_2 monolayer. The structural properties such as bond lengths, bond angles, adsorption energies and Mulliken population analysis and the electronic properties including the density of states and molecular orbitals were also analyzed in detail. The results indicate that the interactions between NH_3 molecules and N-doped TiO_2 in TiO_2-N/MoS_2 nanocomposites are stronger than those between gas molecules and undoped TiO_2 in TiO_2/MoS_2 nanocomposites, which reveals that the N doping helps to strengthen the interaction of NH_3 molecules with hybrid TiO_2/MoS_2 nanocomposites. Therefore, the obtained results also present a theoretical basis for the potential application of TiO_2/MoS_2 nanocomposite as an efficient gas sensor for NH_3 molecule in the environment.

Keywords: *Density Functional Theory; TiO_2; NH_3; TiO_2/MoS_2 nanocomposite; Interaction; Density of states.*

INTRODUCTION

Titania (TiO_2) has aroused eminent interests as one of the most promising semiconductor materials duo to its peculiar properties such as non-toxicity, high catalytic efficiency, extensive band-gap (Satterfield, 1991, Ando, *et al.*, 1997) and chemical stability. TiO_2 has been extensively employed in many fields such as photo-catalysis, manufacturing of gas sensors, development of organic dye-sensitized solar cells and degradation of pollutants (Ando, *et al.*, 1997, Fujishima and Honda, 1972, Dutta, *et al.*, 1999, Garfunkel, *et al.*, 1998). Three important polymorphs of TiO_2 have been identified, namely anatase, rutile, and brookite (Banfied and Veblen, *et al.*, 2015). Anatase and rutile forms are the most widely studied crystalline forms in scientific researches. The wider band gap of TiO_2 (3-3.2 eV) restricts its photocatalytic activity as it can only absorb a lower percentage of the incoming solar light in the ultraviolet region. Upon substituting one oxygen atom of TiO_2 anatase by nitrogen atom, the photocatalytic activity of TiO_2 changes dramatically. This procedure enhances its optical sensitivity to the visible area (Er-

(*) Corresponding Author - e-mail: a_abbasi@azaruniv.edu

dogan, *et al.*, 2010, Zarei, *et al.*, 2013). Two-dimensional (2D) materials, such as molybdenum disulfide (MoS_2) (Helveg, *et al.*, 2000) and other transition metal dichalcogenides such as $MoSe_2$, WS_2 and so on, show the ultimate scaling of material dimension in the vertical direction. MoS_2, a layered structure containing molybdenum and sulfur atoms fascinates many attentions owing to its outstanding electrical, mechanical and optical properties such as fulfilled bandgap, thermal stability, carrier mobility, and so on (Wang, *et al.*, 2012, Kou, *et al.*, 2012, Wei, *et al.*, 2016). MoS2 has been largely utilized in a wide range of applications such as photocatalysts, nanotribology, lithium battery, dry lubrication, hydrodesulfurization catalyst and photovoltaic cell (Lee, 1976, Aruchamy, 1992, Frame and Osterloh, 2012, Li and Galli, 2007). Nanoelectronic devices made-up on 2D materials such as MoS_2 propose also much productivity for these nanostructured materials, resulting in the further miniaturization of the integrated circuits further than Moore's Law. In recent times, several electronic devices have been fabricated by means of few-layer MoS_2 as a main component of nanoelectronic devices such as field effect transistors (Radisavljevic, *et al.*, 2011), sensors (Lembke and Kis, 2012, Li, *et al.*, 2012). Nevertheless, some theoretical investigations of N-doped TiO_2 anatase nanoparticles and layered MoS_2 nanostructures have been published separately, explaining some of the important electronic and structural properties of these materials. Liu and co-workers (Liu, *et al.*, 2012) investigated the molecular NO adsorption on intrinsic and nitrogen-doped TiO_2 anatase nanoparticles. Considering DFT calculations, Liu and co-workers reported that the N-doped TiO_2 anatase nanoparticles react with CO molecules more strongly, compared with the intrinsic nanoparticles (Liu, *et al.*, 2013). Different experimental methods have been employed for synthesizing TiO_2/MoS_2 nanocomposites (Nisar, *et al.*, 2013, Topalian, *et al.*, 2012). The gas sensing capabilities of TiO_2/MoS_2 nanocomposites for the removal of toxic air pollutants have not been studied experimentally or theoretically. NH_3 molecules were characterized as toxic gases. So, controlling the concentrations of these harmful molecules is an important subject to environmental and human health. In this study, the interactions of NH_3 molecules with TiO_2/MoS_2 nanocomposites were investigated by DFT computations. We present here results of calculations of complex systems consisting of NH_3 molecule positioned between the TiO_2 anatase nanoparticle and MoS_2 monolayer. The electronic structures of the adsorption systems have been also analyzed including the projected density of states (PDOS). The main aim of this study is to supply an overall understanding on the adsorption behaviors of nano TiO_2/MoS_2 composites for the elimination of NH_3 molecules.

DETAILS OF COMPUTATIONS AND STRUCTURAL MODELS

Computational Methods

Density Functional Theory computations (Hohenberg and Kohn, 1964, Kohn and Sham, 1965) were performed using the Open source Package for Material eXplorer (OPENMX) ver. 3.8 (Ozaki, *et al.*, 2013), which is assumed to be a powerful software package based on density functional theories, VPS pseudopotantials, and PAO localized basis functions (Ozaki, 2003, Ozaki and Kino, 2005). Pseudo atomic orbitals (PAO's) centered on atomic sites were utilized as basis sets. The cutoff energy of 150 Rydberg was set in these calculations (Ozaki and Kino, 2005). The considered PAO's were created via the basis sets (of three-s, three-p, one-d) for the titanium atom, (of three-s, three-p, two-d) for the molybdenum atom, (of two-s and two-p) for oxygen and nitrogen atoms and (of three-s and three-p) for the sulfur atom. The cutoff radii of basis functions were chosen to be 7 for the titanium atom, 9 for the molybdenum atom, 5 for oxygen and nitrogen atoms and 8 for the sulfur atom. The exchange-correlation energy functional was treated based on generalized gradient approximation (GGA) in the Perdew–Burke–Ernzerhof form (PBE) (Perdew, *et al.*, 1997). The convergence criteria for self-consistent field iterations and energy calculation were set to the values of 1.0×10^{-6} Hartree and 1.0×10^{-4} Hartree/bohr, respectively. The computational effort and accuracy depend on the cutoff energy and the convergence criteria. Since the cutoff energy is not for basis set as in plane wave methods, but for the numerical integrations, the total energy does not have to converge

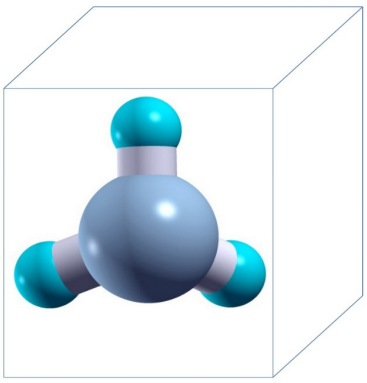

Fig. 1. Representation of NH_3 molecule in a large cubic supercell

from the upper energy region with respect to the cutoff energy like that of plane wave basis set. In most cases, the selected convergence criteria are optimum choices. With the considered values for energy and SCF calculations, the convergence criterion is correctly satisfied. During the optimization of geometrical structures, 'Opt' is used as an efficient geometry optimizer. The open-source program XCrysDen (Koklj, 2003) was used in the display of the considered Figures in this study. The box considered in these computations contains 96 atoms (24 Ti, 48 O, 8 Mo and 16 S atoms) of undoped or N-doped TiO_2 nanoparticle with MoS_2 monolayer. With the chosen sizes of TiO2 and MoS_2, the geometry optimizations were performed properly, giving rise to the convergent results in comparison with the other sizes of nanocomposites. The N-H bond length and H-N-H bond angle of the NH_3 molecule were calculated to be 1.02 Å and 107.8, respectively. Fig. 1 represents the structure of the NH_3 molecule in a cubic The adsorption energy of NH_3 molecule adsorbed on the TiO_2/MoS_2 nanocompopsite was calculated using the following formula:

$$E_{ad} = E_{(composite+adsorbate)} - E_{composite} - E_{adsorbate} \quad (1)$$

where $E_{(composite + adsorbate)}$ and $E_{composite}$ are the total energies of the adsorption system and the TiO_2/MoS_2 nanocomposite, respectively. $E_{adsorbate}$ represents the energy of the isolated NH_3 molecule. $E_{(composite + adsorbate)}$ is estimated from the energy of the entire adsorption system (TiO_2/MoS_2+NH_3) after the relaxation while, $E_{composite}$ and $E_{adsorbate}$ are calculated according to the geometry optimization of the bare TiO_2/MoS_2 and NH_3

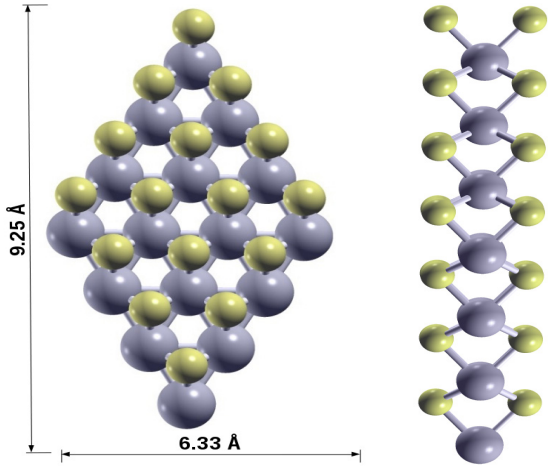

Fig. 2. Optimized structure of the chosen MoS_2 monolayer with area values, (a) Front view and (b) lateral view. Mo atoms are sketched by gray balls and S atoms by yellow balls

molecule, respectively. Based on this definition, the adsorption energies of stable configurations are negative; the more negative the adsorption energy, the more stable the adsorption configuration and consequently more efficient interaction.

Structural models

MoS_2 model: Molybdenum disulfide (MoS_2) is a layered transition metal structure, which belongs to the family of two dimensional dichalcogenides. A hexagonally arrangement of atomic sheets of MoS_2 containing Mo and S atoms set as an S–Mo–S sandwich

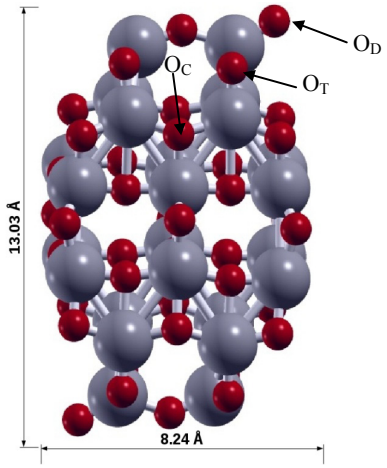

Fig. 3. Optimized structures of undoped 72 atom TiO_2 anatase nanoparticle constructed using the 3×2×1 unit cells; (OC: central oxygen; OT: twofold coordinated oxygen; OD: dangling oxygen). Ti atoms are sketched by dark gray balls, O atoms by red balls and N atoms by blue balls

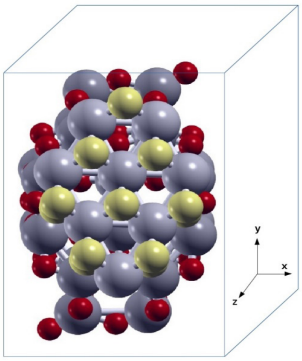

Fig. 4. Optimized structure of the intrinsic TiO_2/MoS_2 nanocomposite constructed from the TiO_2 nanoparticle and MoS_2 monolayer, the dark grey and red balls denote titanium and oxygen atoms, while the light grey and yellow balls represent molybdenum and sulfur atoms, respectively

forms MoS_2 monolayer. The monolayer of MoS_2 model studied here contains 24 atoms in total (8 Mo and 16 S atoms). The structure of MoS_2 monolayer is optimized to obtain the energy minimized structure with optimized structural parameters. The calculated S−Mo bond length, Mo−Mo distance, and S−S distance in monolayer are 2.43 Å, 3.20 Å, and 3.15 Å, respectively. These computed bond lengths are the same as the values of bulk material (Gupta, 1991) in reasonable agreement with the reported data (Li, *et al.*, 2008). The area of the MoS_2 slab is 9.25 Å×6.33 Å. The calculated interlayer distance between MoS_2 layers considered here is only 0.14 Å lower than the experimentally reported result of 6.14 Å for bulk MoS_2 based on GGA functional (Mathur and Baranger, 2001). The optimized structure of MoS_2 model was displayed in Fig. 2.

TiO_2 anatase model: The considered TiO_2 anatase nanoparticles containing 72 atoms were constructed by putting 3×2×1 numbers of TiO_2 unit cells along x, y and z axis, respectively. The unit cell is available at

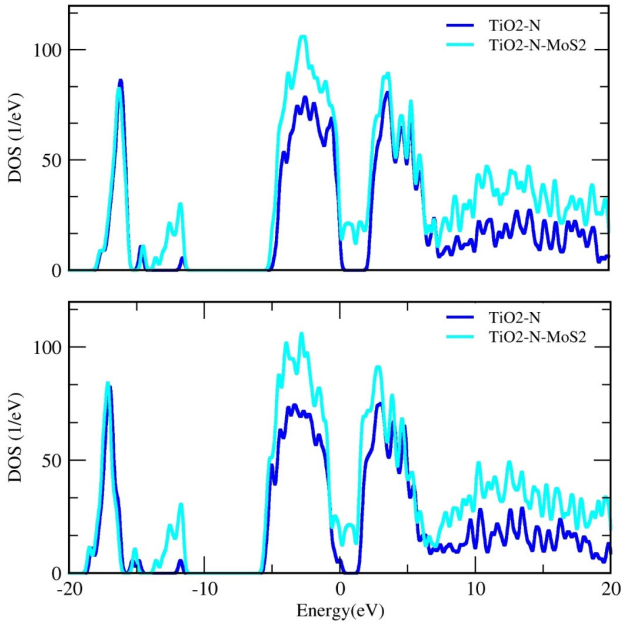

Fig. 6. Total density of states for N-doped TiO_2 and two types of N-doped TiO_2/MoS_2 nanocomposites

"American Mineralogists Database" webpage and was reported by Wyckoff (Wyckoff, 1963). Two appropriate oxygen atoms of TiO_2 nanoparticle were replaced by nitrogen atoms in order to model the N-doped particles. In one doping configuration, a nitrogen atom substitute an oxygen atom in the center of the particle and the other configuration represents the substitution at OT position. The substituted oxygen atoms were denoted by OC and OT in Fig. 3 and correspond to the "central oxygen" and "twofold coordinated oxygen" atoms respectively. The area of the anatase nanoparticle is 13.03 Å×8.24 Å. The crystal model of TiO_2 anatase nanoparticle contains two types of titanium atoms, referred to as five-fold (5f-Ti) and six-fold (6f-Ti), as well as two types of oxygen atoms, specified by three-fold (3f-O) and two-fold (2f-O) O atoms (see Fig. 3) (Wu, *et al.*, 2013). Generally, the

Table 1. Mulliken charge values (|e|) and adsorption energies (eV) of the NH_3 molecule adsorbed on the TiO_2/MoS_2 nanocomposites

Complex	ΔQ (|e|)	ΔE_{ad} (eV)	$E_{(composite + adsorbate)}$	$E_{composite}$
A	-0.110	-1.52	-2233.2	-2202.2
B	-0.160	-1.55	-2233.5	-2202.4
C	-0.180	-1.64	-2236.8	-2196.6
D	-0.185	-1.66	-2237.2	-2196.8
E	-0.105	-0.96	-2124.2	-2204.6

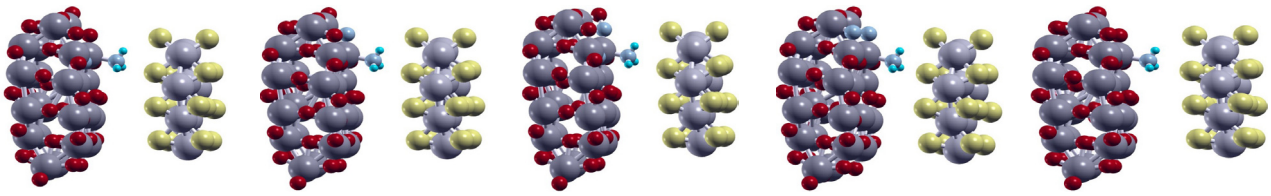

(a) (b) (c) (d) (e)

Fig. 5. Optimized geometry configurations of the interaction of NH_3 molecule with TiO_2/MoS_2 nanocomposites

2f-O and 5f-Ti atoms are more reactive than the 3f-O and f-Ti atoms due to the undercoordination in 2f-O and 5f-Ti atoms. The thickness of the vacuum spacing is 11.5 Å, which is helpful to reduce the interaction between the neighbor particles. The optimized structure of TiO_2/MoS_2 nanocomposite was displayed in Fig. 4.

RESULTS AND DISCUSSION

NH_3 interacts with TiO_2/MoS_2 nanocomposites

The optimized geometry configurations of NH_3 molecule on TiO_2/MoS_2 nanocomposites were presented in Fig. 5. In configurations A and B, NH_3 molecule weakly interacts with the N-doped nanocomposite, while configurations C and D represent the interactions of NH_3 molecule with two-N-doped nanocomposites. Complex E contains the adsorption configuration of NH_3 over the undoped nanocomposite. The results suggest that N-H bonds of the adsorbed NH_3 molecule were stretched after the adsorption process. The reason is that the electronic density transfers from the N-H bonds of the adsorbed NH_3 molecule and the TiO_2 nanocomposite to the newly formed Ti-N bond between the nanocomposite and NH_3 molecule. It means that the N-H bonds are elongated and weakened. The adsorption energy values were listed in Table 1. In this table, the charge difference, ΔQ, is a measure of the amount of charge transferred to, or, from the studied nanocomposites from, or, to the NH_3 molecule. The values of ΔQ for other complexes have negligible differences with this reported value. For example, the calculated Mulliken charge value for N-doped nanocomposite in complex A is -0.11 |e| (e, the electron charge) and that of NH_3 molecule is +0.11 |e|. These values indicate that TiO_2/MoS_2 nanocomposite behaves as an electron acceptor from NH_3 molecule. This structure in the simulation box represents the optimized structure of the nanocomposite after the relaxation. We have placed the TiO_2 nanoparticle in different positions and distances with respect to the MoS_2 nanosheet and obtained the optimized distance between them. In the considered position of the intrin-

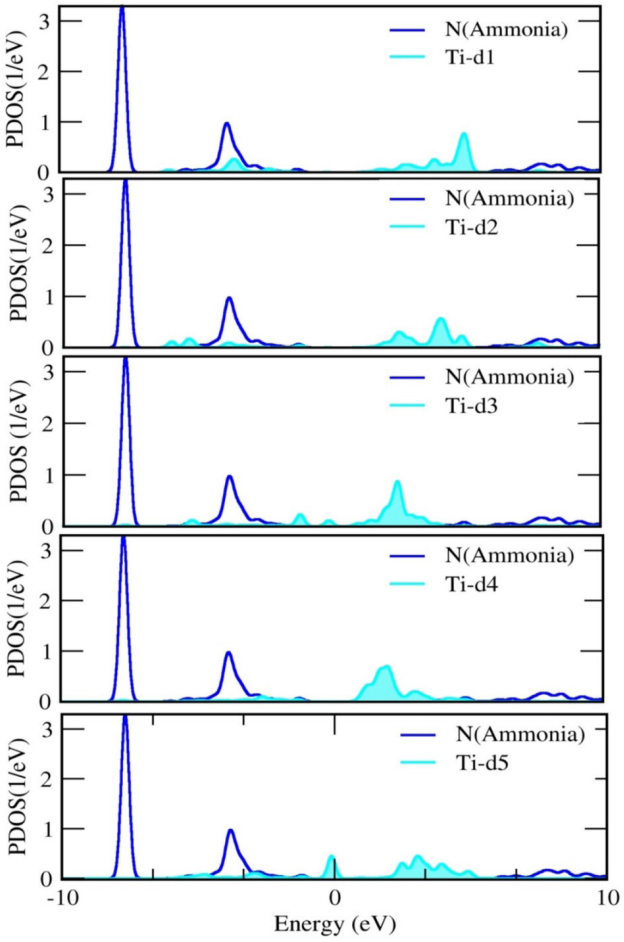

Fig. 7. The PDOSs of the titanium and nitrogen atoms for NH_3 molecule adsorbed on the TiO_2/MoS_2 nanocomposites. HOMO means the highest occupied molecular orbitals and LUMO refers to the lowest unoccupied molecular orbitals, (a) complex A; (b) complex B; (c) complex C; (d) complex D and (e) complex E

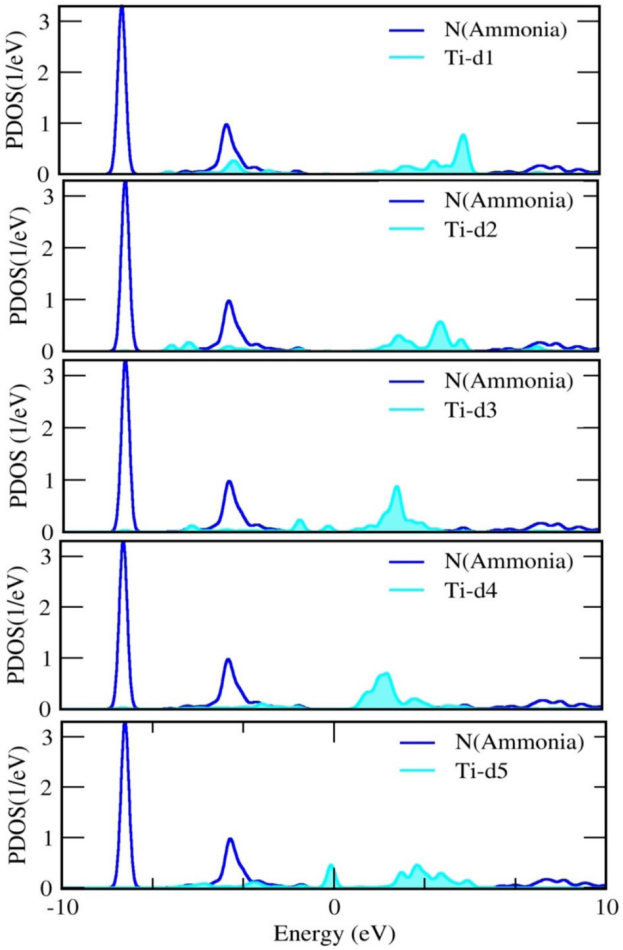

Fig. 8. The PDOSs of the nitrogen atom of the ammonia molecule and the different d orbitals of the titanium atom for NH_3 molecule adsorbed on the TiO_2/MoS_2 nanocomposites

sic TiO_2/MoS_2 nanocomposite, the structure is stable and favorable from the energy point of view. Also, the supercell parameters of the TiO_2 and MoS_2 in this position match reasonably with the parameters of the bulk material. That is the reason that the structure is considered as the optimized geometric structure of TiO_2 and MoS_2, forming efficient nanocomposite after relaxation.

The configurations depicted in Fig.5 differ in the position of the doped nitrogen atom into the TiO_2 nanoparticle, as well as the number of doped nitrogen atoms. For example, complex A represents the OC-substituted TiO_2 and MoS_2 monolayer with adsorbed NH_3 molecule, whereas complex B shows the OT-substituted nanocomposite and NH_3. Complexes C and D represent the OC, T-substituted nanocomposites with adsorbed NH_3 molecule. Complex E also depicts the structure of the pristine TiO_2/MoS_2 nanocomposite

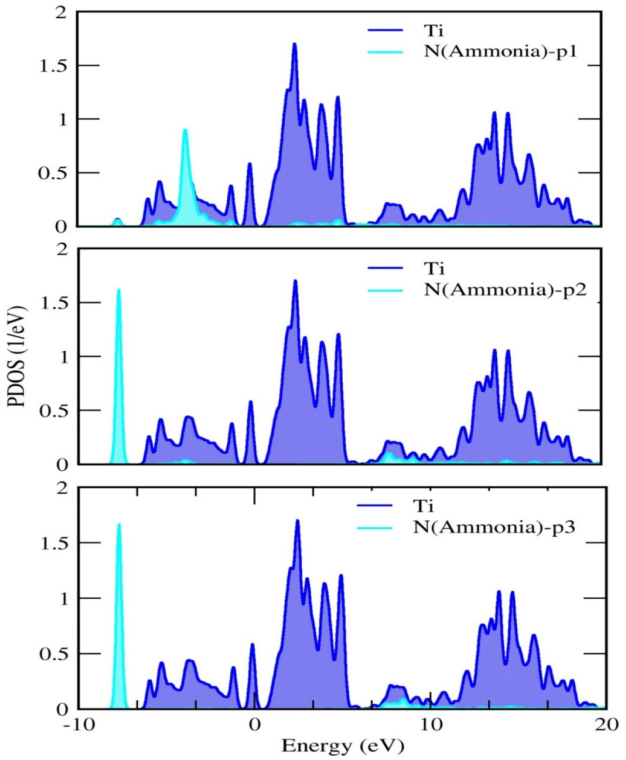

Fig. 9. The PDOSs of the titanium atom of the TiO_2 nanoparticle and different p orbitals of the of the nitrogen atom of the ammonia molecule for complex A

and NH_3 molecule adsorbed to it.

The adsorption energy of NH_3 molecule over the N-doped nanocomposite is higher (more negative) than that of undoped nanocomposite, suggesting that the interaction of NH_3 molecule with N-doped nanocomposites is energetically more favorable than the interaction with the pristine ones. Besides, two-N-doped nanocomposite adsorbs NH_3 molecule more strongly compared with the N-doped and undoped ones. This is due to the higher adsorption energy of two-N-doped nanocomposite in comparison with the N-doped and pristine ones. Therefore, the N-doped nanoparticles have higher sensing capabilities than the undoped ones for NH_3 detection. The interaction with two-N-doped nanocomposites leads to the most stable and most energy favorable adsorption configurations. Thus, the N doping helps to strengthen the adsorption of the NH_3 molecule on the considered nanocomposites. To fully examine the interaction of NH_3 molecules with the considered nanocomposites, we have performed density of states analysis for the studied systems. The open source program, Xmgrace, was used in the calculation of the density of states.

The "cube" files obtained from the calculations using Open MX software are converted and imported to the Xmgrace database. The software will calculate automatically the DOS and PDOS plots using the data provided in the "cube" files. Fig. 6 represents the total DOS for two types of N-doped TiO_2 anatase nanoparticles and corresponding TiO_2/MoS_2 nanocomposites. Panel (a) represents the DOS of OC-substituted TiO_2/MoS_2 nanocomposite, while panel (b) displays that of OT-substituted one.

The shifting of the energy of the states is seen for nanocomposites in comparison with the isolated TiO_2 nanoparticles. Fig. 7 displays the PDOSs of the titanium and nitrogen atoms after the adsorption on the TiO_2/MoS_2 nanocomposites.

Panels (a-e) in this Fig. represent the PDOSs of the titanium and nitrogen atoms for complexes A-E, indicating significant overlaps between the PDOSs of the titanium and nitrogen atoms. These high overlaps in the PDOSs of titanium and nitrogen atoms represent the formation of new chemical Ti-N bond between the nanocomposite and NH_3 molecule. The PDOSs of the nitrogen atom of ammonia molecule and different d orbitals of the titanium atom were shown in Fig. 8.

As can be seen from this Fig., there is a considerable overlap between the PDOSs of the nitrogen atom and d1 orbital of the titanium. This result confirms the strong interaction of the nitrogen atom of ammonia molecule and d1 orbital of the titanium atom. Fig. 9 presents the PDOSs of the titanium atom of the nanoparticle and three p orbitals of the nitrogen atom of the ammonia molecule.

A close inspection of this Fig. reveals the highest overlap between the PDOSs of the titanium atom and the p1 orbital, compared to the other p orbitals.

CONCLUSIONS

First principles calculations were performed to examine the ammonia interactions with TiO_2/MoS_2 nanocomposites. Ammonia molecule preferentially interacts with fivefold coordinated titanium atoms of TiO_2 nanoparticle. The results suggest that the N-H bonds of NH_3 molecule are weakened after the interaction. The results also suggest that the N-doped nanocomposites have a higher efficiency to adsorb toxic NH_3 molecule on their surfaces than the pristine ones. Analysis of the adsorption energies reveals that the interaction of the NH_3 molecule with N-doped nanocomposites is energetically more favorable than the interaction with undoped ones. In other words, the N-doped nanocomposite adsorbs NH_3 molecule more strongly comparing with the pristine one. Besides, two-N-doped nanocomposite is more sensitive than the N-doped and undoped nanocomposites for NH_3 detection in the environment. The calculation of the Mulliken charges and density of states indicate the sensitivity of the considered nanocomposites in the presence of NH_3 molecule. The charge analysis reveals a considerable charge transfer from the NH_3 to the nanocomposite. The strong adsorption of NH_3 on the N-doped nanocomposites represents the higher sensing capability of the TiO_2/MoS_2 nanocomposites for NH_3 recognition in the environment. Our theoretical results here suggest that the N-doped nanocomposite would be an ideal NH_3 gas sensor and remover.

ACKNOWLEDGEMENT

This work was supported by the Azarbaijan Shahid Madani University.

REFERENCES

Satterfield, C.N., (1991). Heterogeneous catalysis in industrial practice. 2nd ed., McGraw-Hill, New York.

Ando, M.; Kobayashi, T.; Haruta, M., (1997). Combined effects of small gold particles on the optical gas sensing by transition metal oxide films. J. Catal. Today, 36: 135-141.

Fujishima, A.; Honda, K., (1972). Electrochemical photolysis of water at a semiconductor electrode. Nature, 37: 238-242.

Dutta, P.K.; Ginwalla, A.; Hogg, B.; Patton, B.R.; Chwieroth, B.; Liang, Z.; Gouma, P.; Mills, M.; Akbar, S., (1999). Interaction of carbon monoxide with anatase surfaces at high temperatures: optimization of a carbon monoxide sensor. J. Phys.

Chem. B, 103: 4412-4422.

Garfunkel, E.; Gusev, E.; Vul, (Eds.) A., (1998). Fundamental aspects of ultrathin dielectrics on Si-based devices, NATO Science Series, Kluwer Academic Publishers, Dordrecht.

Banfied, J.F.; Veblen, D.R., (1992). Conversion of Perovskite to Anatase and TiO_2 (B): A TEM Study and the Use of Fundamental Building-Blocks for Understanding Relationship among the TiO_2 Minerals Am. Mineral., 77: 545-557.

Erdogan, R.; Ozbek, O.; Onal, I., (2010). A periodic DFT study of water and ammonia adsorption on anatase TiO_2 (001) slab. Surf. Sci., 604: 1029-1033.

Zarei, H.; Zeinali, M.; Ghourchian, H.; Eskandari, Kh., (2013). Gold nano-particles as electrochemical signal amplifier for immune-reaction monitoring. Int. J. Nano. Dimens, 4(1): 69-76.

Helveg, S.; Lauritsen, J.V.; Lægsgaard, E.; Stensgaard, I.; Nørskov, J.K.; Clausen, B.S.; Topsøe, H.; Besenbacher, F., (2000). Atomic-Scale Structure of Single-Layer MoS_2 Nanoclusters, J. Phys. Rev. Lett., 84: 951−954.

Wang, H.; Yu, L.; Lee, Y.H.; Shi, Y.; Hsu, A.; Chin, M.L.; Li, L.J.; Dubey, M.; Kong, J.; Palacios, T., (2012). Integrated Circuits Based on Bilayer MoS_2 Transistors, Nano Lett., 12: 4674−4680.

Kou, L.; Tang, C.; Zhang, Y.; Heine, T.; Chen, C.; Frauenheim, T., (2012). Tuning Magnetism and Electronic Phase Transitions by Strain and Electric Field in Zigzag MoS_2 Nanoribbons, J. Phys. Chem. Letts., 3: 2934-2941.

Wei, W.; Dai, Y.; Huang, B., (2016). In-plane interfacing effects of two-dimensional transition-metal dichalcogenide heterostructures, Phys. Chem. Chem. Phys., DOI: 10.1039/C6CP02741E.

Lee, P.A., (1976). Physics and Chemistry of Materials with Layered Structures: Optical and Electrical Properties; Reidel: Dordrecht, The Netherlands.

Aruchamy, A., (1992). Ed.;Photochemistry and Photovoltaics of Layered Semiconductors; Kluwer: Dordrecht, The Netherlands.

Frame, F.A.; Osterloh, F.E., (2010). CdSe-MoS2: A quantum size-confined p CdSe-MoS_2: A quantum size-confined photocatalyst for hydrogen evolution from water under visible light, J. Phys. Chem. C, 114: 10628-10633.

Li, T.S.; Galli, G.L., (2007). Electronic properties of MoS_2 nanoparticles, J. Phys. Chem. C, 111: 16192−16196.

Radisavljevic, B.; Radenovic, A.; Brivio, J.; Giacometti, V.; Kis, A., (2011). Single-layer MoS2 transistors, Nat. Nanotechnol., 6: 147−150.

Lembke, D.; Kis, A., (2012). Breakdown of High-Performance Monolayer MoS_2 Transistors, ACS nano., 6: 10070-10075.

Li, H.; Yin, Z.; He, Q.; Li, H.; Huang, X.; Lu, G.; Fam, D.W.H.; Tok, A.I.Y.; Zhang, H., (2012). Fabrication of Single-and Multilayer MoS_2 Film-Based Field-Effect Transistors for Sensing NO at Room Temperature, Small., 8(1): 63-67.

Liu, J.; Liu, Q.; Fang, P.; Pan, C.; Xiao, W., (2012). First principles study of the adsorption of a NO molecule on N-doped anatase nanoparticles. J. Appl. Surf. Sci., 258: 8312-8318.

Liu, J.; Dong, L.; Guo, W.; Liang, T.; Lai, W., (2013). CO adsorption and oxidation on N-doped TiO_2 nanoparticles, J. Phys. Chem. C, 117: 13037-13044.

Nisar, J.; Topalian, Z.; Sarkar, A.D.; Österlund, L.; Ahuja, R., (2013). TiO_2-Based Gas Sensor: A Possible Application to SO_2, ACS Appl. Mater. Interfaces, 5 (17): 8516–8522.

Topalian, Z.; Niklasson, G.A.; Granqvist, C.G.; Österlund, L., (2012). Spectroscopic Study of the Photofixation of SO_2 on Anatase TiO_2 Thin Films and Their Oleophobic Properties, ACS Appl. Mater. Interfaces, 4 (2): 672–679.

Hohenberg, P.; Kohn, W., (1964). Inhomogeneous electron gas. J. Phys. Rev., 136: B864-B871.

Kohn, W.; Sham, L., (1965). Self-Consistent equations including exchange and correlation effects. J. Phys. Rev., 140: A1133-A1138.

The code, OPENMX, pseudoatomic basis functions, and pseudopotentials are available on a web site 'http://www.openmxsquare.org'.

Ozaki, T., (2003). Variationally optimized atomic orbitals for large-scale electronic structures. Phys. Rev. B, 67: 155108.

Ozaki, T.; Kino, H., (2004). Numerical atomic basis orbitals from H to Kr, J. Phys. Rev. B, 69: 195113.

Perdew, J.P.; Burke, K.; Ernzerhof, M, (1997). Gen-

eralized gradient approximation made simple, J. Phys. Rev. Lett., 78: 1396.

Koklj, A., (2003). Computer graphics and graphical user interfaces as tools in simulations of matter at the atomic scale, J. Comput. Mater. Sci., 28: 155-168.

Gupta, T.K., (1991). Preparation and characterization of layered superconductors, J. Phys. Rev. B, 43: 5276−5279.

Li, Y.F.; Zhou, Z.; Zhang, S.B.; Chen, Z.F., (2008). MoS_2 nanoribbons: high stability and unusual electronic and magnetic properties, J. Am. Chem. Soc., 130: 16739−16744.

Mathur, H.; Baranger, H.U., (2001). Random Berry phase magnetoresistance as a probe of interface roughness in Si MOSFET's, J. Phys. Rev. B, 64: 235325.

Wyckoff, R.W.G., (1963). Crystal structures, Second edition. Interscience Publishers, USA, New York.

Wu, C.; Chen, M.; Skelton, A.A.; Cummings, P. T.; Zheng, T., (2013). Adsorption of Arginine–Glycine–Aspartate Tripeptide onto Negatively Charged Rutile (110) Mediated by Cations: The Effect of Surface Hydroxylation, J. ACS Appl. Mat. Interface, 5: 2567.

AUTHOR (S) BIOSKETCHES

Amirali Abbasi, PhD Candidate, Molecular Simulation Laboratories (MSL), Azarbaijan Shahid Madani University, Tabriz, Iran & Computational Nanomaterials Research Group, Azarbaijan Shahid Madani University, Tabriz, Iran & Chemistry Department, Faculty of Basic Sciences, Azarbaijan Shahid Madani University, Tabriz, Iran, *Email: a_abbasi@azaruniv.edu*

Jaber Jahanbin Sardroodi, Associate Professor, Molecular Simulation Laboratories (MSL), Azarbaijan Shahid Madani University, Tabriz, Iran & Computational Nanomaterials Research Group, Azarbaijan Shahid Madani University, Tabriz, Iran & Chemistry Department, Faculty of Basic Sciences, Azarbaijan Shahid Madani University, Tabriz, Iran